Available online at www.sciencedirect.com

ScienceDirect

Ceramics International 40 (2014) 2299–2304

CERAMICS INTERNATIONAL

www.elsevier.com/locate/ceramint

Phase formation, microstructure and magnetic properties of $(1-x)BiFeO_3$–$x(0.9Pb(Mg_{1/3}Nb_{2/3})O_3$–$0.1PbTiO_3)$ system

Rewadee Wongmaneerung[a,*], Pongsakorn Jantaratana[b], Rattikorn Yimnirun[c], Supon Ananta[d]

[a]*Faculty of Science, Maejo University, Chiang Mai 50290, Thailand*
[b]*Department of Physics, Kasetsart University, Bangkok 10900, Thailand*
[c]*School of Physics, Institute of Science, Suranaree University of Technology, and NANOTEC-SUT Center of Excellence on Advanced Functional Nanomaterials, Nakhon Ratchasima 30000, Thailand*
[d]*Department of Physics and Materials Science, Faculty of Science, Chiang Mai University, Chiang Mai 50200, Thailand*

Received 18 July 2013; received in revised form 30 July 2013; accepted 30 July 2013
Available online 7 August 2013

Abstract

Multiferroic composites containing bismuth ferrite (BF) and lead magnesium niobate–lead titanate (0.9PMN–0.1PT) phases were fabricated by solid-state reaction, with 10–50 wt% of 0.9PMN–0.1PT. The phase formation behavior and microstructural features were investigated by X-ray diffraction (XRD) and scanning electron microscopy (SEM), respectively. Information on the oxidation state of Fe ions was determined by the synchrotron X-rays absorption near edge structure (XANES) technique. A vibrating sample magnetometer (VSM) was used to characterize the magnetic properties. The results indicated that all composites showed a perovskite structure and the PMN–PT phase was compatible with the BF phase. The microstructure displayed mixed BF, PMN and PT phases. In addition, the presence of secondary phases ($Bi_2Fe_4O_9$ and Fe_2O_3) was observed by both XRD and XANES techniques. The presence of BF, $Bi_2Fe_4O_9$ and Fe_2O_3 phases was also confirmed by the oxidation state and the local structure surrounding the Fe absorbing atom, as observed in the Fe K-edge XANES spectrum. Moreover, the composites exhibited typical magnetic hysteresis (M–H) loops at room temperature. The maximum saturation magnetization (M_S) was observed for $x=30$ and 40 wt%.

Keywords: B. Composites; C. Magnetic properties; Multiferroic; $BiFeO_3$-based ceramics

1. Introduction

Perovskite solid-solutions have been an active area of research due to their importance in ferroelectric, ferromagnetic and piezoelectric applications along with their fascinating physical properties [1–3]. In particular, Bi-based ferroelectrics are under intense investigation because of their multiferroic properties, i.e. ferroelectricity with high Curie temperature (T_C) [4] and antiferromagnetic properties below Néel temperature (T_N) [5]. However, the choice of single-phase materials exhibiting coexistence of strong ferro-ferrimagnetism and ferroelectricity is limited. Therefore, the composite concept has been proposed.

The emergence of a new class of two-phase materials, namely, multiferroic composites (ferroelectric–ferromagnetic or dielectric–ferromagnetic composites) has attracted wide attention from academics and industries because these composites are desirable for the synthesis of materials with unique or improved properties. The sum properties of the composites, e.g. dielectric properties, ferroelectric properties, electrical conductivity, ferromagnetic properties, density, etc., are also equally important as they affect the product's properties and hence its application in various practical devices.

Multiferroic $BiFeO_3$ (BF) shows antiferromagnetic G-type spin configuration along the $[111]_c$ or $[111]_h$ directions in its pseudocubic or rhombohedral structure. Interestingly, this ferromagnetic BF exhibits characteristic features in dielectric properties around the magnetic transition temperature, highlighting useful multiferroic behavior [6]. Moreover, BF compound is one of the ferro-electromagnetic multiferroics, in which ferroelectric ($T_C=830$ °C) and antiferromagnetic ($T_N=370$ °C) [4–7] order parameters co-exist up to quite high temperature. One of the main obstacles for BF applications is

*Corresponding author. Tel.: +66 53 873515; fax: +66 53 878225.
E-mail address: re_nok@yahoo.com (R. Wongmaneerung).

0272-8842/$ - see front matter © 2013 Elsevier Ltd and Techna Group S.r.l. All rights reserved.
http://dx.doi.org/10.1016/j.ceramint.2013.07.151

large leakage current. Recently, for high temperature applications and to solve the above problems, a binary system of multiferroic composites has been widely studied [8–10]. In the present research report, an attempt has been made to study a ternary system, $BiFeO_3$–$Pb(Mg_{1/3}Nb_{2/3})O_3$–$PbTiO_3$, aiming at the development of multiferroic materials with desirable magnetic properties and with reduction in leakage current. $PbTiO_3$ (PT) was employed to form multiferroic composites with BF to improve the electro-magnetic properties because of its high ferroelectric transition temperature, large polarization and strong ability to stabilize the perovskite phase [11,12]. In addition, $Pb(Mg_{1/3}Nb_{2/3})O_3$ (PMN) has not yet been explored in multiferroic composites.

2. Experimental

The $(1-x)$BF–x(0.9PMN–0.1PT) (where x=10, 20, 30, 40 and 50 wt%) composite materials were prepared by standard ceramic method. Firstly, laboratory grade reagents of Bi_2O_3 and Fe_2O_3 were used to prepare the $BiFeO_3$ ferrite phase. The $Pb(Mg_{1/3}Nb_{2/3})O_3$ and $PbTiO_3$ ferroelectric phases were synthesized from high purity oxides of PbO, MgO, Nb_2O_5 and TiO_2 powders. BF, PMN and PT powders were prepared separately. The constituent BF compounds in suitable stoichiometry were thoroughly mixed in a ball mill for 24 h, while PMN and PT phases were milled by vibro-milling for 1 h. The $BiFeO_3$ ferrite and $Pb(Mg_{1/3}Nb_{2/3})O_3$ and $PbTiO_3$ ferroelectric phases were calcined separately at 850, 950 and 600 °C for 2 h, respectively. Multiferroic composites of $(1-x)$BF–x(0.9PMN–0.1PT) were prepared by milling in a ball-mill for 24 h. The composite powders were pressed into disc pellets 10 mm in diameter and 1.5 mm in thickness using uniaxial pressing. The pellets were sintered at 800 and 900 °C for 2 h in air.

X-ray diffraction patterns of the composites were recorded by an X-ray powder diffractometer with Cu K_α radiation at room temperature. The local structure around the Fe ions of the samples was obtained by X-ray absorption near edge structure (XANES) technique. XANES measurements at the Fe K-edge were performed with synchrotron radiation in fluorescence mode at the Synchrotron Light Research Institute, Nakhon Ratchasima, Thailand, using beamline BL8. The microstructure of composites was examined with a field emission scanning electron microscope (FE-SEM) in backscattering electron mode. The magnetic data was recorded with the help of a vibrating sample magnetometer (VSM) by applying an external magnetic field of 8 kOe at room temperature.

3. Results and discussion

The typical X-ray diffraction patterns of $(1-x)$BF–x(0.9PMN–0.1PT) multiferroic composites with sintering temperature at 800 and 900 °C are shown in Figs. 1 and 2, respectively. It is clearly seen that ferrite and ferroelectric phases are identified in composites. All the reflection peaks were indexed using the observed inter-planar spacing (d) The observed d values of all diffraction lines of $(1-x)$BF–x

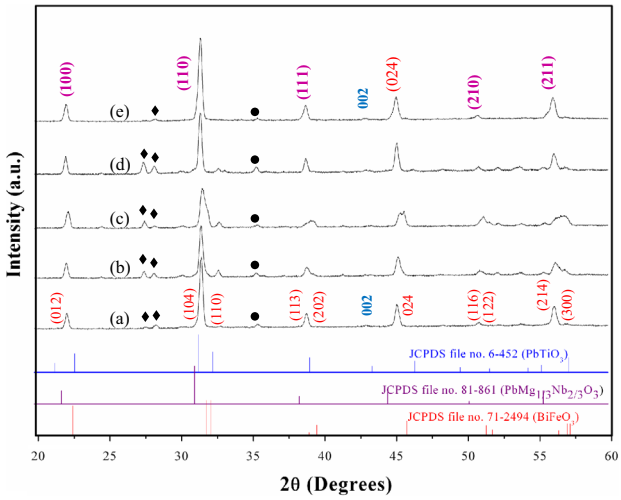

Fig. 1. XRD patterns of $(1-x)$BF–x(0.9PMN−0.1PT) multiferroic composites sintered at 800 °C with (a) 10, (b) 20, (c) 30, (d) 40 and (e) 50 wt% of 0.9PMN−0.1PT.

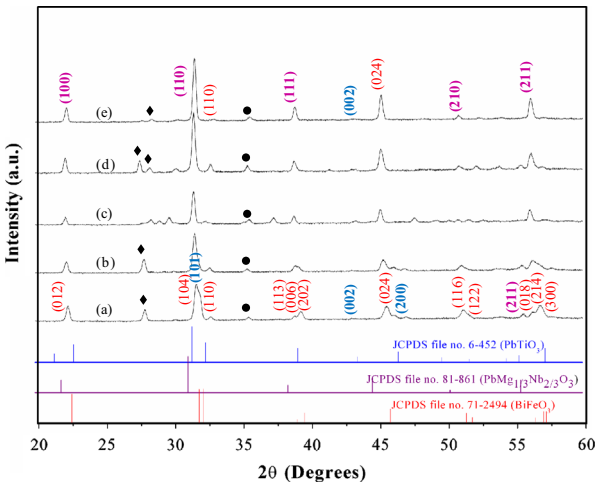

Fig. 2. XRD patterns of $(1-x)$BF–x(0.9PMN–0.1PT) multiferroic composites sintered at 900 °C with (a) 10, (b) 20, (c) 30, (d) 40 and (e) 50 wt% of 0.9PMN–0.1PT.

(0.9PMN–0.1PT) composites with different x content suggest that there is a change in the crystal structure from rhombohedral to mixed cubic–tetragonal. A comparison between the XRD patterns reveals that the intensity of 0.9PMN–0.1PT peaks increases with increasing percentage of PMN–PT in these composites, while the intensity of ferrite peaks is reduced continuously. As shown in Figs. 1(b) and 2(b), the strongest diffraction peaks (104)(110) of BF shift toward lower angles for the composites. In Fig. 2, it is especially evident that the splitting peaks (006)(200) shift toward lower angles and become one diffraction peak (111). This may be explained by the fact that the radius of Pb^{2+} (119 pm) is larger than that of Bi^{3+} (103 pm), and that the radii of Mg^{2+} (72 pm), Nb^{5+} (64 pm) and Ti^{4+} (61 pm) are larger than that of Fe^{3+} (49 pm) [13], resulting in an increase of unit cell volume with a shift of diffraction peaks toward lower angles. However, the secondary phases ($Bi_2Fe_4O_9$ (♦) and Fe_2O_3 (●)) are formed during the

firing process. In particular, the minor $Bi_2Fe_4O_9$ phase can be clearly seen at higher sintering temperature (900 °C) due to the decomposition of BF phase at high temperature [14]. As seen in Figs. 1 and 2, when 0.9PMN–0.1PT content increases, the amount of BF decreases and $Bi_2Fe_4O_9$ and Fe_2O_3 also decrease. The increase of 0.9PMN-0.1PT and decrease of BF, $Bi_2Fe_4O_9$ and Fe_2O_3 cause a reduction in magnetic properties.

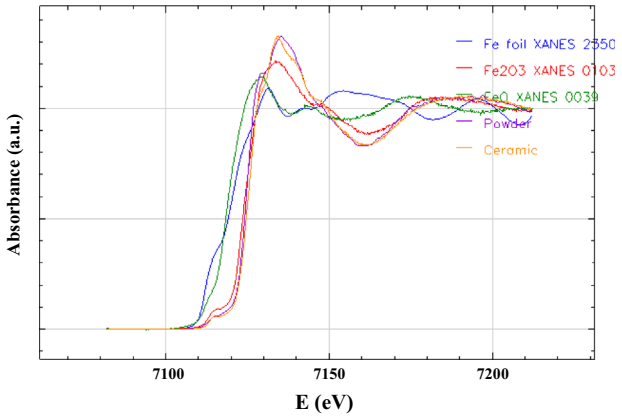

Fig. 3. Fe K-edge XANES spectra of 0.7BF–0.3(0.9PMN–0.1PT) powders and ceramic compare with the Fe K-edge XANES spectra of Fe, Fe_2O_3 and FeO standard.

The Fe K-edge X-ray absorption spectra of 0.7BF–0.3 (0.9PMN–0.1PT) samples are shown in Fig. 3, compared with the spectra of Fe foil, Fe_2O_3 (Fe^{3+}) and FeO (Fe^{2+}) standards. The high local sensitivity of XANES technique allows better structural characterization of the supported phases. After usual background removal and normalization, the normalized data were analyzed in the XANES region between 7050 and 7250 eV. The excited energy (E_0) for $0.7BF-0.3(0.9PMN–0.1PT)$ powders and ceramic were 7137 and 7135 eV, respectively. These E_0 values are closer to the E_0 value of Fe_2O_3 standard. This clearly indicated that the oxidation state of Fe ions in the composite sample contained Fe^{3+}, confirming that Fe in the samples are in the form of BF, $Bi_2Fe_4O_9$ and Fe_2O_3, as Fe ions in these three compounds is surrounded by 6 O ions (FeO_6) [15–17].

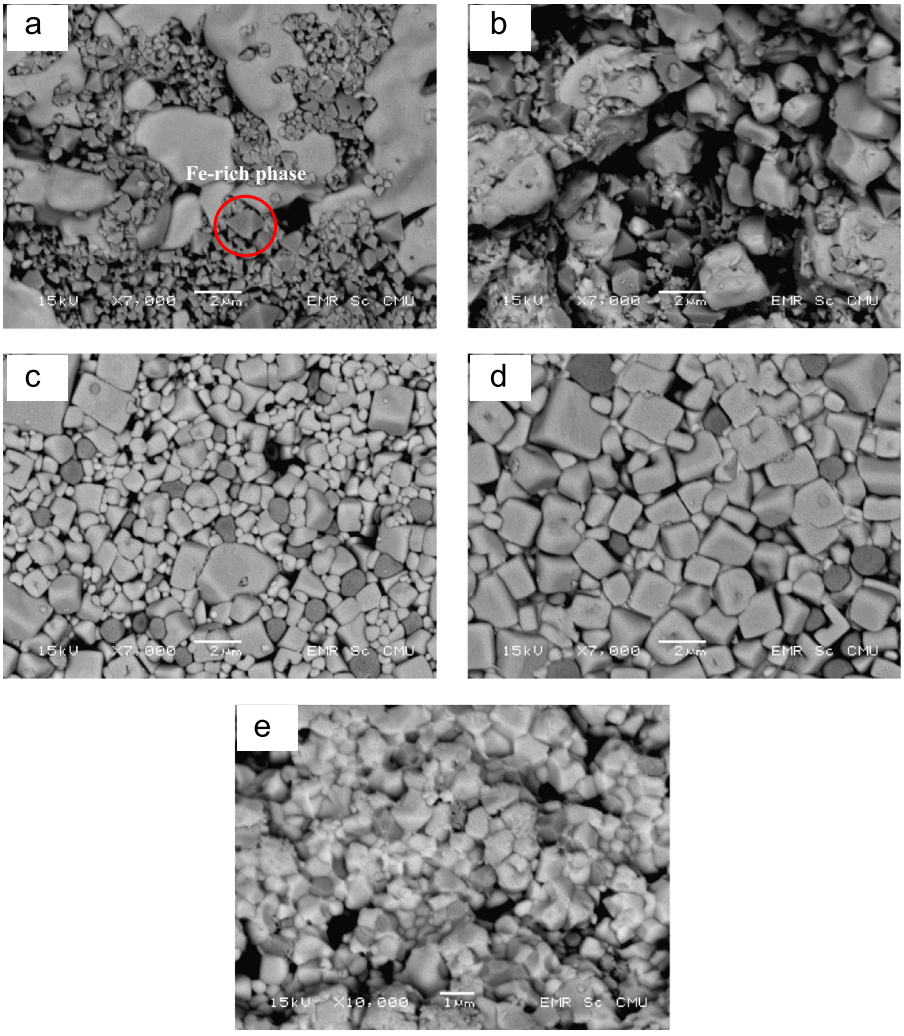

Fig. 4. SEM micrographs of $(1-x)$BF–x(0.9PMN–0.1PT) multiferroic composites sintered at 800 °C with (a) 10, (b) 20, (c) 30, (d) 40 and (e) 50 wt% of 0.9PMN–0.1PT.

The backscattered electron images of composite samples with various compositions are shown in Figs. 4 and 5 (sintered at 800 and 900 °C, respectively). Since the composites are multiphase, it is desirable to know the distribution of the constituent phases observed in the microstructure. It should be noted that the overall microstructure of composites sintered at 800 and 900 °C is totally different from those observed in the case of BF-based solid-solution [18,19]. As a result, the microstructure became non-uniform. When more than 30 wt % of 0.9PMN–0.1PT was added to BF, there were major changes in the microstructure, as shown in Fig. 4(c)–(e). A uniform microstructure can be seen. In the images, the dark colored grains are ferrite grains and the light colored ones are PMN–PT ferroelectric grains. It is clear that two component phases co-exist in the sintered composites. It can also be observed that the grain sizes of the two phases vary with the relative content of the components. Moreover, the grain sizes of PMN–PT and BF are found to be different; ferrite grains are 0.5–1.25 μm in size, while PMN–PT grain size varies in the range of 1.0–3.75 μm. The average grain size of the ferroelectric phase is larger than that of ferrite phase in these composites. However, there are some large pores and agglomeration of the ferrite particles. These can be found in the composites containing 10 and 20 wt% of PMN–PT.

In addition to BF matrix phase, two secondary phases were identified by XRD, $Bi_2Fe_4O_9$ and Fe_2O_3. These two phases were observed within the composite samples. Energy-dispersive X-ray spectroscopy (EDS) analysis confirmed that the irregular-shaped dark regions are essentially Fe_2O_3. The lighter colored grains are probably the $Bi_2Fe_4O_9$ phase. For higher-temperature sintering, a pronounced second phase is segregated at the grain boundaries. The observation of these layers could be attributed to a liquid-phase formation during the sintering process, as proposed by several researchers [20,21]. Uneven grain boundaries are also observed in Fig. 4 (a) and (e). This uneven grain boundary seems to be a diffusion induced grain boundary migration [22]. In general, this mechanism is evidence of the chemical composition gradient; therefore, dissolution of Fe^{3+} ions from ferrite into ferroelectric phase can be expected in this composition. In this

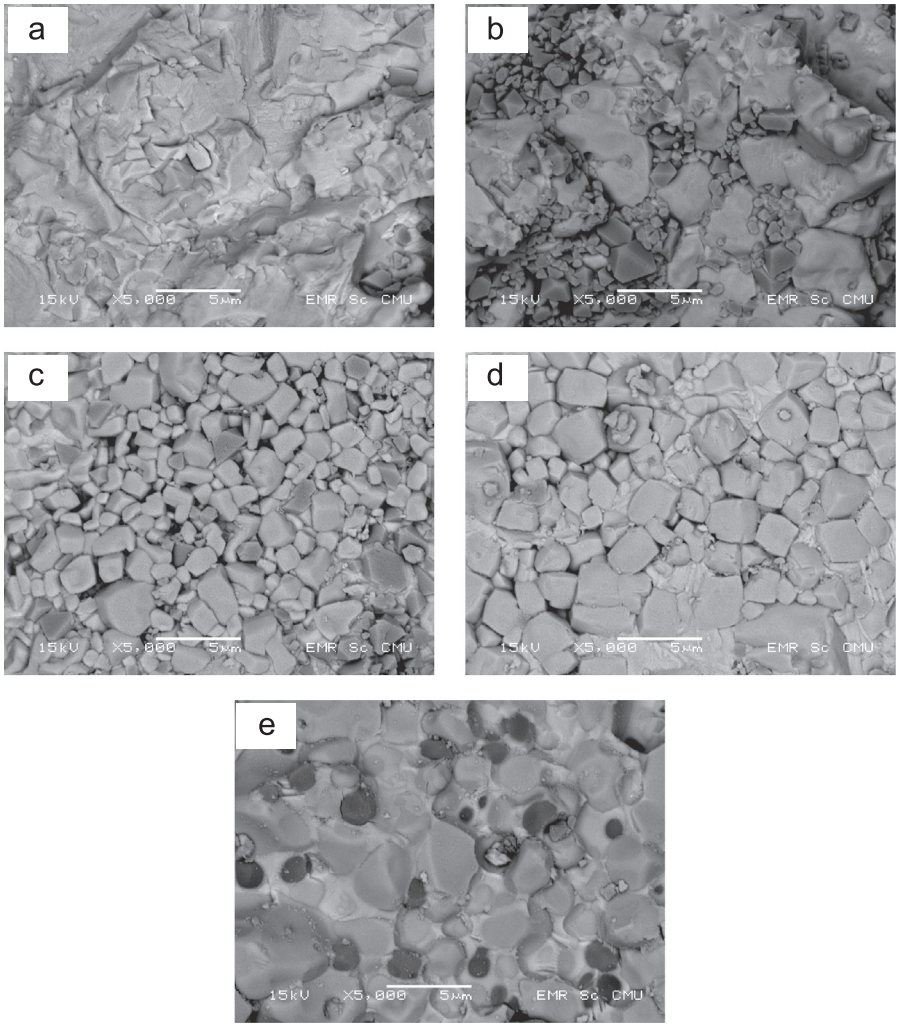

Fig. 5. SEM micrographs of $(1-x)$BF–x(0.9PMN–0.1PT) multiferroic composites sintered at 900 °C with (a) 10, (b) 20, (c) 30, (d) 40 and (e) 50 wt% of 0.9PMN–0.1PT.

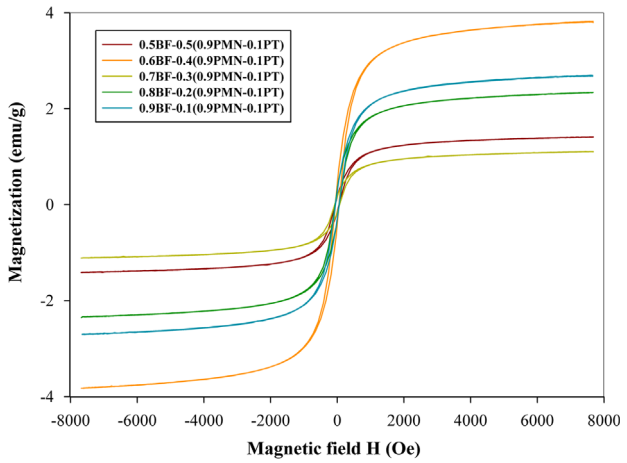

Fig. 6. *M–H* hysteresis loops of $(1-x)$BF–x(0.9PMN–0.1PT) multiferroic composites sintered at 800 °C.

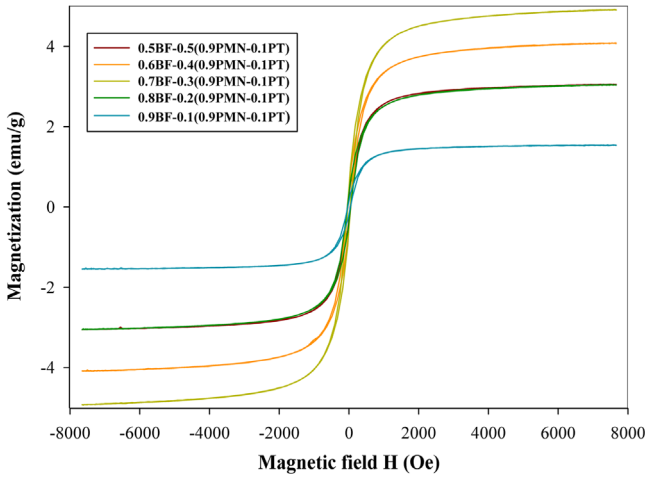

Fig. 7. *M–H* hysteresis loops of $(1-x)$BF–x(0.9PMN–0.1PT) multiferroic composites sintered at 900 °C.

work, the connectivity was not controlled, the actual connectivity was a random mixture of 3–0 and 0–3 connectivity [23].

The magnetic hysteresis (*M–H*) loops of BF–PMN–PT composites were investigated at room temperature using a VSM with an applied magnetic field of $-8\ \text{kOe} \le H \le 8\ \text{kOe}$, as shown in Figs. 6 and 7 for samples sintered at 800 and 900 °C, respectively. The magnetic properties of materials are usually characterized by a hysteresis loop, which determines the behavior of materials when excited by an external magnetic field. Moreover, the magnetic characteristics of the composites follow from the ferrite's properties, which are sensitive to composition, processing and firing conditions. If the presence of a ferroelectric in these composites does not change the intrinsic magnetic properties of the BF phase, a proportional reduction in the sum magnetization of composites with a reduction in the amount of the ferrite phase, is expected. From the graphs, it is noted that composites exhibit a typical magnetic hysteresis, indicating that the composites in the BF–PMN–PT system are magnetically ordered. All compositions show ferromagnetic behavior, unlike BF which is an antiferromagnetic material. The BF–PMN–PT samples also exhibit very narrow ferromagnetic hysteresis loops, which can be attributed to the size effect [24]. The magnetic behavior of small sized grains of antiferromagnetic materials was first proposed by Néel in 1961 [25]. Moreover, it is also possible that this behavior arises from mixed phases between BF, $Bi_2Fe_4O_9$ and Fe_2O_3, because BF material shows antiferromagnetic properties [5], $Bi_2Fe_4O_9$ is paramagnetic [16] and Fe_2O_3 exhibits weak ferromagnetic behavior [26] at room temperature. It is observed that the magnetization hysteresis loop of the sample sintered at 900 °C is almost identical to that of the sample sintered at 800 °C. This could be attributed to the magnetic contribution of the impurity phases present in the samples. In all ferromagnetic samples, saturation is achieved at 8 kOe, with values in the range of 0.9–3.3 emu/g (1.4–4.6 emu/g) for samples sintered at 800 °C (900 °C). For $x=10$, the saturation magnetization is 2.45 (1.46) emu/g; for $x=20$, 30, 40 and 50, values of 2.10 (2.82), 0.97 (4.67), 3.28 (3.86) and 1.26 (2.84) emu/g, respectively, are obtained. These values are significantly larger than the value of ~0.2 emu/g for pure BF [11]. The saturation magnetization (M_S) of the composites decreases with an increase in "x"

In addition, according to XRD results (Figs. 1 and 2), as the amount of 0.9PMN–0.1PT increases, the amounts of BF, $Bi_2Fe_4O_9$ and Fe_2O_3 decrease. The decrease in these three compounds also has a strong effect on the magnetic behavior, as the M_s is clearly reduced. This behavior can be attributed to structural distortion in the perovskite: i.e. the spin arrangement of unpaired electrons on Fe^{3+} ions is caused by the incorporation of Pb^{2+} ions into A sites and/or Mg^{2+}, Nb^{5+} and Ti^{4+} ions into B sites of the perovskite structure of BF [27]. Another possible reason is that by introduction a given amount of 0.9PMN–0.1PT, the spin structure of BF may be broken resulting in a reduction in M_S and weak ferromagnetic behavior. This results in a decrease of magnetic parameters with increasing 0.9PMN–0.1PT concentration in multiferroic composites (Table 1)

4. Conclusions

Composite materials consisting of $BiFeO_3$ as a ferrite phase and $0.9Pb(Mg_{1/3}Nb_{2/3})O_3$–$0.1PbTiO_3$ as a ferroelectric phase have been synthesized successfully using solid–state reaction method. The coexistence of BF and PMN–PT phases in these composites has been confirmed by XRD analysis and SEM images. The sintered composites consist of secondary phases of $Bi_2Fe_4O_9$ and Fe_2O_3, which strongly affect the magnetic properties. The phase structure changes from rhombohedral to mixed cubic–tetragonal phase as the content of 0.9PMN–0.1PT increases. SEM observations reveal that the co–existence of two phases affects the sintering and grain growth behavior of the components. These composites show typical magnetic behavior, which is found to change from antiferromagnetic to weak ferromagnetic. Moreover, the saturation

Table 1
Magnetic properties of (1–*x*)BF–*x*(0.9PMN–0.1PT) multiferroic composites.

Sintering temperature (°C for 2 h)	Composition (*x*) (weight fraction)	Magnetic properties		
		Ms (emu/g)	*Mr* (emu/g)	*Hc* (Oe)
800	10	2.45	0.39	55.36
	20	2.10	0.30	62.90
	30	0.97	0.17	72.97
	40	3.28	0.62	50.33
	50	1.26	0.19	60.39
900	10	1.46	0.18	47.81
	20	2.82	0.39	55.36
	30	4.67	0.57	42.78
	40	3.86	0.51	52.84
	50	2.84	0.33	40.26

magnetization values are found to decrease with increasing PMN–PT content.

Acknowledgments

The authors would like to thank the Thailand Research Fund (TRF) and the Faculty of Science, Maejo University, for financial support.

References

[1] R.E. Cohen, Origin of ferroelectricity in perovskite oxides, Nature 358 (1992) 136–138.
[2] L. Bellaiche, A. Garcia, D. Vanderbilt, Finite-temperature properties of $Pb(Zr_{1-x}Ti_x)O_3$ alloys from first principles, Physical Review Letter 84 (2000) 5427–5430.
[3] I. Grinberg, V.R. Cooper, A.M. Rappe, Relationship between local structure and phase transitions of a disordered solid solution, Nature 419 (2002) 909–911.
[4] G.A. Smolenskii, V.A. Isupov, A.I. Agranovskaya, N.N. Krainik, New ferroelectrics of complex composition, Soviet Physics Solid State 2 (1961) 2651–2654.
[5] G.A. Smolenskii, V.M. Yudin, E.S. Sher, Y.E. Stolypin, Antiferromagnetic properties of some perovskites, Soviet Physics JETP 16 (1963) 622–624.
[6] R. Mazumder, P. Sujatha Devi, D. Bhattacharya, P. Choudhury, A. Sen, M. Raja, Ferromagnetism in nanoscale $BiFeO_3$, Applied Physics Letter 91 (2007) 062510–062513.
[7] S.P. Solov'ev, Y.N. Venevtsev, G.S. Zhdanov, An X-ray study of phase transitions in $NaNbO_3$, Soviet Physics Crystallography 6 (1961) 171–175.
[8] Y. Zhou, J. Zhang, L. Li, Y. Su, J. Cheng, S. Cao, Multiferroic composites in nano-microscale with non-solid solution by Co-ferrite and $(K_{0.5}Na_{0.5})NbO_3$-based ferroelectric matrix, Journal of Alloys and Compounds 484 (2009) 535–539.
[9] S. Narendra Babu, K. Srinivas, T. Bhimasankaram, Studies on lead-free multiferroic magnetoelectric composites, Journal of Magnetism and Magnetic Materials 321 (2009) 3764–3770.
[10] V. Corral–Flores, D. Bueno-Baqués, R.F. Ziolo, Synthesis and characterization of novel $CoFe_2O_4$–$BaTiO_3$ multiferroic core–shell-type nanostructures, Acta Materialia 58 (2010) 764–769.
[11] K. Singh, N.S. Negi, R.K. Kotnala, M. Singh, Dielectric and magnetic properties of $(BiFeO_3)_{1-x}(PbTiO_3)_x$ ferromagnetoelectric system, Solid State Communications 148 (2008) 18–21.
[12] W.M. Zhu, Z.-G. Ye, Effects of chemical modification on the electrical properties of $0.67BiFeO_3-0.33PbTiO_3$ ferroelectric ceramics, Ceramics International 30 (2004) 1435–1442.
[13] R.D. Shannon, Revised effective ionic radii and systematic studies of interatomic distances in halides and chalcogenides, Acta Crystallographica A 32 (1976) 751–767.
[14] T.T Carvalho, P.B. Tavares, Synthesis and thermodynamic stability of multiferroic $BiFeO_3$, Materials Letter 62 (2008) 3984–3986.
[15] J. Lu, A. Günther, F. Schrettle, F. Mayr, S. Krohns, P. Lunkenheimer, A. Pimenov, V.D. Travkin, A.A. Mukhin, A. Loidl, On the room temperature multiferroic $BiFeO_3$: magnetic, dielectric and thermal properties, European Physical Journal B 75 (2010) 451–460.
[16] J. Zhao, T. Liu, Y. Xu, Y. He, W. Chen, Synthesis and characterization of $Bi_2Fe_4O_9$ powders, Materials Chemistry and Physics 128 (2011) 388–391.
[17] J. Zhang, Z.Y. Wu, K. Ibrahim, M.I. Abbas, X. Ju, Surface structure of α-Fe_2O_3 nanocrystal observed by O K-edge X-ray absorption spectroscopy, Nuclear Instruments and Methods in Physics Research B 199 (2003) 291–294.
[18] M. Mahesh Kumar, S. Srinath, G.S. Kumar, S.V. Suryanarayana, Spontaneous magnetic moment in $BiFeO_3$–$BaTiO_3$ solid solutions at low temperatures, Journal of Magnetism and Magnetic Materials 188 (1998) 203–212.
[19] F. Prihor Gheorghiu, A. Ianculescu, P. Postolache, N. Lupu, M. Dobromir, D. Luca, L. Mitoseriu, Preparation and properties of $(1-x)BiFeO_{3-x}BaTiO_3$ multiferroic ceramics, Journal of Alloys and Compounds 506 (2010) 862–867.
[20] H.C. Wang, W.A. Schulze, Order–disorder phenomenon in lead scandium tantalate, Journal of the American Ceramic Society 73 (1990) 825–832.
[21] S.M. Gupta, A.R. Kulkarni, Role of excess PbO on the microstructure and dielectric properties of lead magnesium niobate, Journal of Materials Research 10 (1995) 953–961.
[22] J.K. Park, D.Y. Kim, Effect of grain size on diffusion-induced grain-boundary migration in $Ba(Zn_{1/3}Nb_{2/3})O_3$ ceramics, Journal of the American Ceramic Society 79 (1996) 1405–1408.
[23] R.E. Newnham, Composite electroceramics, Ferroelectrics 68 (1986) 1–32.
[24] T.–J. Park, G.C. Papaefthymiou, A.J. Viescas, A.R. Moodenbaugh, S.S. Wong, Size-dependent magnetic properties of single-crystalline multiferroic $BiFeO_3$ nanoparticles, Nano Letter 7 (2007) 766–772.
[25] L. Neel, Superparamagnétisme des grains très fins antiferromagnétiques, Comptes Rendus 252 (1961) 4075–4080.
[26] Z.H. Jing, S.H. Wu, Preparation and magnetic properties of spherical α-Fe_2O_3 nanoparticles via a non-aqueous medium, Materials Chemistry and Physics 92 (2005) 600–603.
[27] R. Rai, A.L. Kholkin, S. Sharma, Multiferroic properties of $BiFeO_3$ doped Bi $(MgTi)O_3$–$PbTiO_3$ ceramic system, Journal of Alloys and Compounds 506 (2010) 815–819.